Geometry and Stability of Be_nC_m ($n = 1-10$; $m = 1, 2, ...,$ to $11 - n$) Clusters

Mohammed M. Ghouri,[†] Lakshmi Yareeda,[†] and Daniela S. Mainardi*[,†,‡]

Institute for Micromanufacturing and the Chemical Engineering Program, Louisiana Tech University, Ruston, Louisiana 71272

Received: July 26, 2007; In Final Form: September 13, 2007

Density functional theory B3PW91/6-31+G* calculations on Be_nC_m ($n = 1-10$; $m = 1, 2, ...,$ to $11 - n$) clusters have been carried out to examine the effect of cluster size, relative composition, binding energy per atom, HOMO−LUMO gap, vertical ionization potential, and electron affinity on their relative stabilities. The most stable planar cyclic conformations of these clusters always show at least a set of two carbon atoms between two beryllium atoms, while structures where beryllium atoms cluster together, or allow the intercalation of one carbon atom between two of them, generally seem to be the least stable ones. Clusters containing 1, 2, and 3 beryllium atoms (Be_2C_8, Be_3C_6, Be_2C_6, BeC_6, Be_2C_4, BeC_4, Be_2C_2, and BeC_2) are identified as clusters of "magic numbers" in terms of their high binding energy per atom, high HOMO−LUMO gap, vertical ionization potential, and second difference in energy per beryllium atom.

1. Introduction

Over the past decade, a lot of emphasis has been paid to the study of the physical and the chemical properties of atomic clusters,[1−3] which are aggregates of atoms containing from a few to a few thousand atoms.[4] These clusters are known to exhibit strong size-dependent effects and display properties that are significantly different from those of their bulk structures due to a quite large surface-to-volume ratio.[4] The emergence of new research areas such as nanoscience and nanotechnology and their promise of different possible technological applications have further fueled the interest in cluster systems. Main issues in cluster science focus on determining their size-evolutionary patterns based on the clusters' unique conformations and stabilities in terms of their energy-related properties. For instance, shell models relate to the formation of "magic clusters" corresponding to closure of electronic or nuclear shells in clusters, which correlates with enhanced energetic stability.[4−7] The discovery of clusters with special geometry and stability formed by "magic" number of atoms is one of the goals of cluster science, because those interesting units can be used to further assemble more complex materials. Extensive theoretical calculations have been conducted to examine structure, energetics, and stability of small clusters[8−13] and to explore the potential to assemble crystals from them.[14−22]

Experimental determinations of the ground state and isomeric conformations of clusters are currently subtle issues mainly due to practical difficulties in applying structure determination techniques such as photoelectron spectroscopy (PES) to such systems. PES provides information about the electronic structure and excitation energies of atomic clusters; however, a difficulty in applying PES to cluster systems is the need for size selectivity due to size resolution issues.[23] Hence, many studies on the electronic structure of clusters have been focused on size-selected neutral clusters,[24] such as As_2, As_4, and P_4,[25] and the photodetachment of negatively charged clusters.[26,27] Theoretical studies, however, allow detailed investigation of ground states and their higher-energy isomers that may appear to be the preferred stable structures at particular operating conditions. Hence, comparison of experimental PES data with theoretical calculations has become a valuable means to determine the structures and low-lying isomers for a variety of clusters.[28−33] Thus, theoretical and experimental studies of clusters are very useful for the understanding of electronic, chemical, and physical properties and prediction of the cluster local chemistry.[33] In particular, theoretical methods based on solutions to the Schrödinger equation[34−36] provide accurate characterization of cluster structures.

Many studies have been performed on small pure carbon clusters[37−44] and carbon-containing clusters.[8,45−48] Moreover, because they form the basic structural units of new materials with potential applications, for instance, in astrochemistry/physics,[49] heteroatom-doped carbon clusters have been a topic of many theoretical investigations.[49,50] Recently, much attention has been paid to the study of beryllium-doped carbon clusters because the addition of beryllium provides a means to stabilize the highly reactive linear carbon chains for applications in astrophysics.[51−54] This particular interest yielded to the extensive theoretical investigations of heteroatom-doped carbon clusters of the form C_nBe^{2-} ($n = 4-14$),[51] BeC_{2n}^{2-} ($n = 2-6$),[52] and BeC_n^- ($n = 1-8$),[53] because these species were particularly observed experimentally.[54] Chen et al.[51] performed density functional theory (DFT) calculations on C_nBe^{2-} ($n = 4-14$) using the B3LYP method in combination with the 6-31G* basis set and found that the ground state structures of the clusters are linear chains with the beryllium atom located inside the C_n chain. Zhang[52] studied BeC_{2n}^{2-} ($n = 2-6$) at the hybrid B3LYP functional and 6-311+G(2df) theory level and reported that linear chains correspond to the ground states of metastable $C_2BeC_2^{2-}$ and highly stable $C_2BeC_4^{2-}$, $C_4BeC_4^{2-}$, $C_4BeC_6^{2-}$, and $C_6BeC_6^{2-}$ clusters. In a more recent study, Chen et al.[53] investigated BeC_n^- ($n = 1-8$) clusters using B3LYP/6-311+G*//B3LYP/6-31G* theory levels and found that these clusters with even n are more stable than the ones with odd n. They attribute such an even/odd alternation in the stabilities of

* Author to whom correspondence should be addressed. E-mail: mainardi@latech.edu.
† Institute for Micromanufacturing.
‡ The Chemical Engineering Program.

10.1021/jp075931c CCC: $37.00
Published on Web 11/20/2007

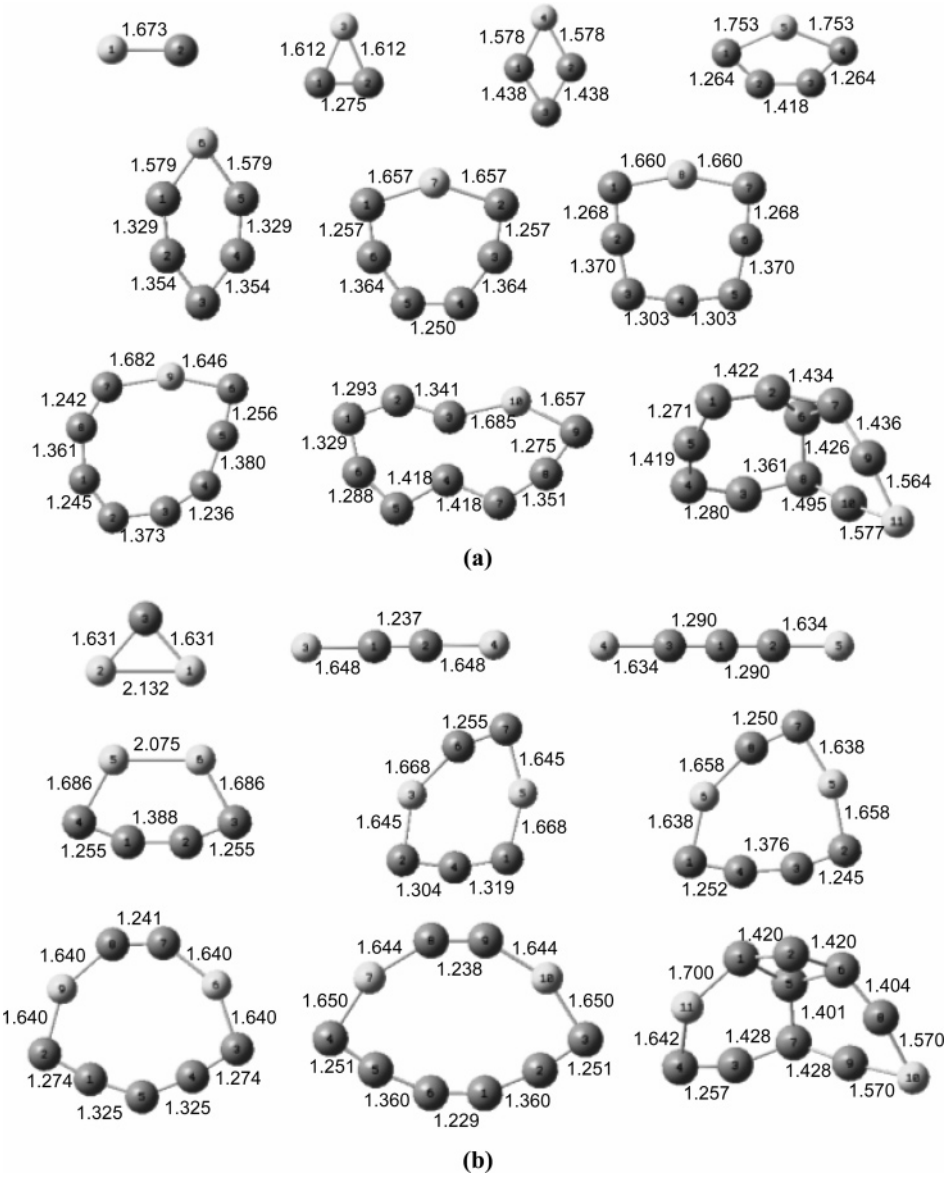

Figure 1. Calculated ground state conformations and selective bond lengths of (a) BeC_m ($m = 1-10$) and (b) Be_2C_m ($m = 1-9$) neutral clusters. Light and dark gray balls represent beryllium and carbon atoms, respectively. Distances are in angstroms.

these systems to trends observed in the local positive charge of the Be atom, electron affinity, variations in bond lengths, incremental binding energy, and dissociation channels.[53]

Not only ionic carbon−heteroatom cluster systems were worthy of extensive research. With the discovery of the metallocarbohedrenes (Metcars) of the form M_mC_n, where M is any metal (mostly a transition metal) by Castleman and coworkers,[55−57] carbon−metal and also carbon−nonmetal neutral systems have been investigated comprehensively.[58−61] In particular, studies with different carbon−"nonmetal" clusters such as carbon−nitrogen[46] and carbon−silicon[8,62] have been the focus of attention for applications in astrophysics[48,63] and electronics,[8] respectively. Belbruno et al.[46] studied the structural stability and the energetics of up to 12-atom clusters of C−N using the density functional B3LYP in combination with the cc-PVTZ basis set. These authors confirmed at that theory level that linear carbon chains with the nitrogen atoms at the terminal positions are the global minima (ground states) of C−N structures with one or two nitrogen atoms. They predicted that this is the case for up to a total number of 13 carbon atoms and contrasted this with the pure carbon clusters, where the cyclic rings are energetically favorable when the cluster size is 9 or greater.[40] Pradhan and Ray[8] studied the electronic properties and the geometrical structures of small carbon−silicon clusters of the form Si_mC_n ($1 \le m, n \le 4$; $n \le m$). Using DFT local density approximation (LDA) in conjunction with the 6-311++G** basis set, these authors reported that the Si_3C_3 cluster is a candidate for a "magic" cluster with a very high stability based on their reported electronic properties, such as the HOMO−LUMO gaps, vertical ionization potentials (IP_v's), and the vertical electron affinities (EA_v's). They also reported that the clusters with equal numbers of silicon and carbon atoms tend to be particularly stable.[8]

The discovery of carbon nanotubes[64] and other carbon-related nanostructures such as fullerenes[65] has taken the interest in carbon and its related clusters even further. Of particular importance is the potential hydrogen storage capacity of carbon-based nanostructures.[66] For instance, fullerenes have a limited capacity to hold a certain number of endohedral substituents depending on their sizes. However, in some cases, the insertion of dopants such as lithium[67] or beryllium[68] have shown promise for enhanced hydrogen storage capacity of carbon-doped nanostructures. Hence, alkali-metal-doped[69,70] and alkaline-earth-metal-doped,[71] especially beryllium-doped carbon nanostruc-

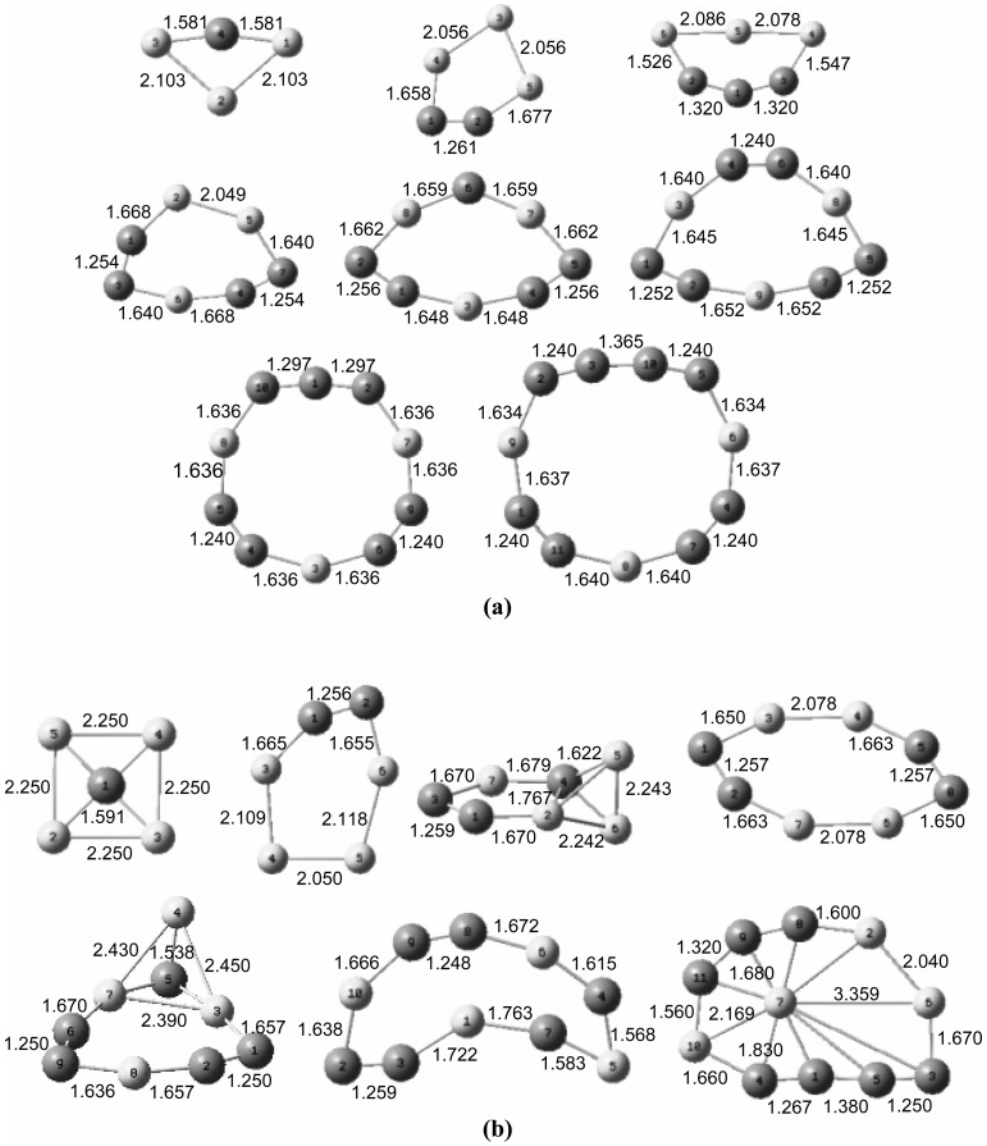

Figure 2. Same as Figure 1 for (a) Be_3C_m ($m = 1-8$) and (b) Be_4C_m ($m = 1-7$) neutral clusters.

tures,[68,72] are considered to be likely candidates for hydrogen storage materials. Metal hydrides are also being considered for hydrogen storage applications.[73] In particular, lithium−beryllium hydrides are the lightest reversible complex metal hydrides with promising gravimetric hydrogen storage capacities (more than 8 wt %);[74] however, the high temperature needed for hydrogen desorption (∼150 °C) is a major drawback.[74] The possibility of using carbon as a dopant in such hydrides might reduce the temperature for hydrogen desorption, as clearly happens in the case of magnesium hydrides,[75,76] making the Li−Be−C hydrides attractive complex metal hydrides for hydrogen storage applications. The interest of this study is, therefore, to advance the knowledge of structure and energetics of Be−C neutral clusters for the prediction of highly stable "magic" clusters with potential use in diverse technological applications such as hydrogen storage. Therefore, it is of fundamental importance to study the size dependence of electronic and geometric structures of Be−C clusters as functions of both particle size and composition. In this paper, a systematic study on the neutral beryllium−carbon clusters of the form Be_nC_m ($n = 1-10$; $m = 1, 2, ...,$ to $11 - n$) is performed. According to this notation, for each n value, $1 \leq n \leq 10$, m can take the values 1, 2, ..., up to $11 - n$. It is expected that the fundamental study presented in this work will lead to a better understanding of the bulk beryllium−carbon nanostructures and therefore aid in tailoring novel materials for such aforementioned applications.

2. Computational Methods

Density functional theory calculations of Be_nC_m $n = 1-10$, $m = 1, 2, ...,$ to $11 - n$ neutral (zero total charge) clusters are performed using the Gaussian '03 program, revision C.02.[77] A large variety of possible geometrical arrangements of these clusters are investigated, including three-dimensional (3-D), cyclic, and linear configurations where n beryllium and m carbon atoms are placed in different ways that they can group. The density functional employed in these calculations is the B3-PW91, one of the most successful hybrid functionals,[78] which includes an exchange description constituted by contributions of local, nonlocal (Becke three-parameter), and Hartree−Fock exchange terms, and correlation given by the 1991 Perdew and Wang (PW91) nonlocal generalized gradient approximation functional.[34] This DFT method is used in combination with the 6-31+G* basis set, which is a split-valence double-ζ that considers d-like polarization functions on heavy atoms and a set of diffuse s- and p-like functions on heavy atoms.[34]

The B3PW91 method is known to perform very well on the structure and stability of pure Be[79,80] and C clusters.[81] For

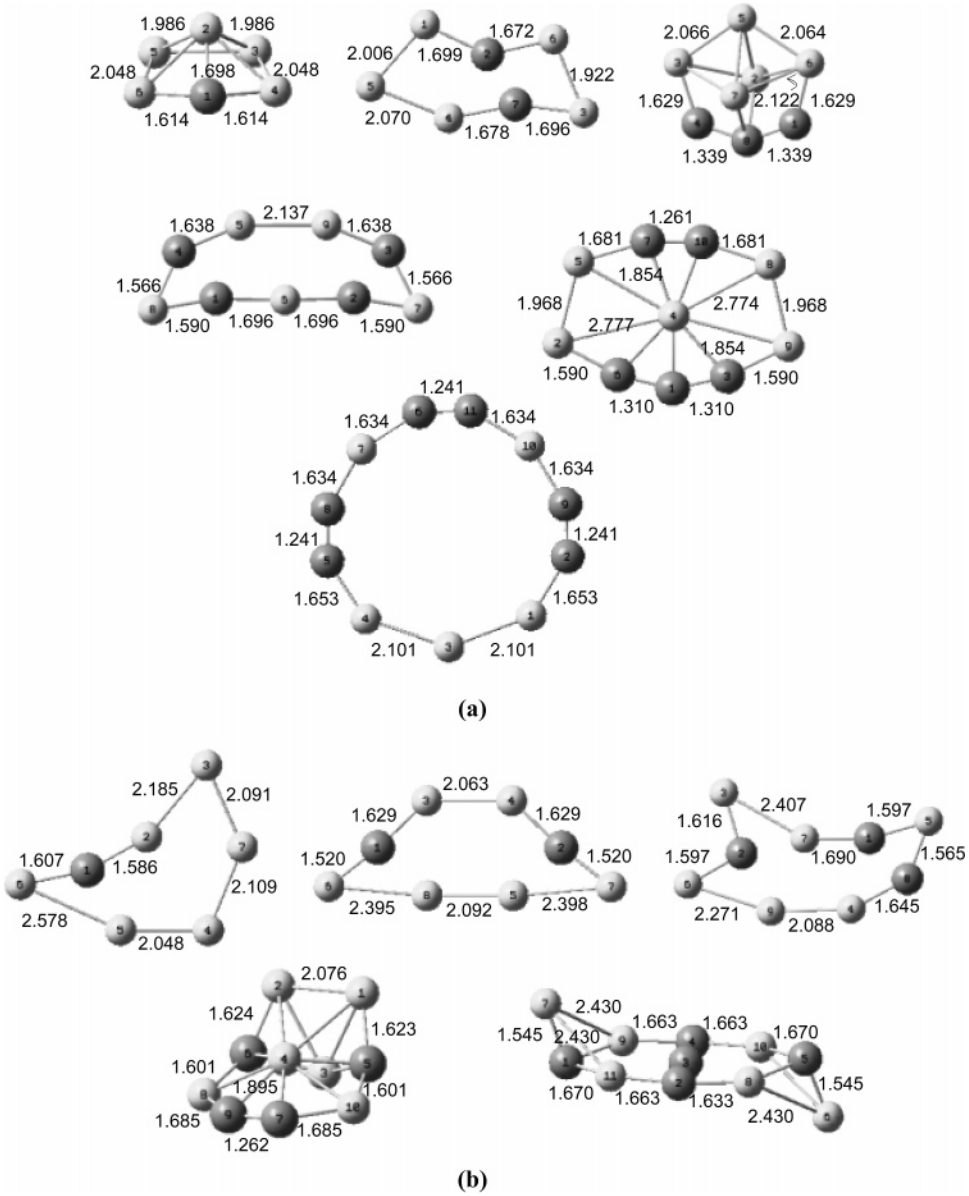

Figure 3. Same as Figure 1 for (a) Be_5C_m ($m = 1-6$) and (b) Be_6C_m ($m = 1-5$) neutral clusters.

instance, Zhao et al.[80] studied the structure and stability of Be_6, Be_6^+, and Be_6^- clusters using B3PW91, B3LYP, and MP2 levels in combination with the 6-311G* and 6-311+G* basis sets. They have also used CCSD(T)/6-311+G* to check the reliability of the results when the calculations at the aforementioned levels contradicted each other. In particular, these authors correctly predicted using the B3PW91, MP2, and CCSD(T) methods that the ground state configuration of Be_6 is a D_{2h} structure, also well-predicted by Pacchioni and Koutecký[82] using pseudopotential configuration interaction (CI). At the B3LYP level of theory, however, Zhao et al. found that the D_{2h} structure is a transitional state instead of a local minimum and that the most stable configuration of Be_6 is wrongly predicted to be a D_{3d} structure, which was also reported by Beyer et al.[83] at the B3LYP/6-311++G (3df) level as the most stable one for Be_6. Similar conclusions are drawn by the same authors for Be_5 in terms of the comparable performance of the B3PW91, MP2, and CCSD(T) methods.[79] Structure and stability of pure carbon clusters have been extensively studied.[37−44,81] In particular, Martin et al.[81] showed that the B3PW91 DFT method reproduces couple cluster CCSD(T) isomerization energies much better than the B3LYP counterpart and the MP2 method, which is known to produce fictitious results for carbon clusters.[81] Hence, the B3PW91/6-31+G* theory level is further used in this work for the prediction of accurate geometric and reliable energetics of Be_nC_m clusters for which electron correlation effects are very important. When this theory level is used, errors in calculated bond lengths (Å) and absolute energies (hartree) are expected to be in the third and fifth decimal, respectively.[84]

Geometry optimizations and harmonic vibrational frequency calculations for all of the 55 Be_nC_m $n = 1-10$, $m = 1, 2, ...,$ to $11 - n$ neutral ground state clusters, 38 different spin multiplicity ($2S + 1$) state clusters, and 113 isomers are performed to ensure that stationary points on the potential energy surface of the clusters are in fact local minima. Spin multiplicity states are checked in all calculations, and ground state geometries as well as stable higher-energy isomers are presented. Zero-point corrected absolute energies are used for further calculation of binding energies and second differences in energy.

3. Results and Discussion

3.1. Ground State Conformations. Ground state structures of the 55 Be_nC_m $n = 1-10$, $m = 1, 2, ...,$ to $11 - n$ neutral

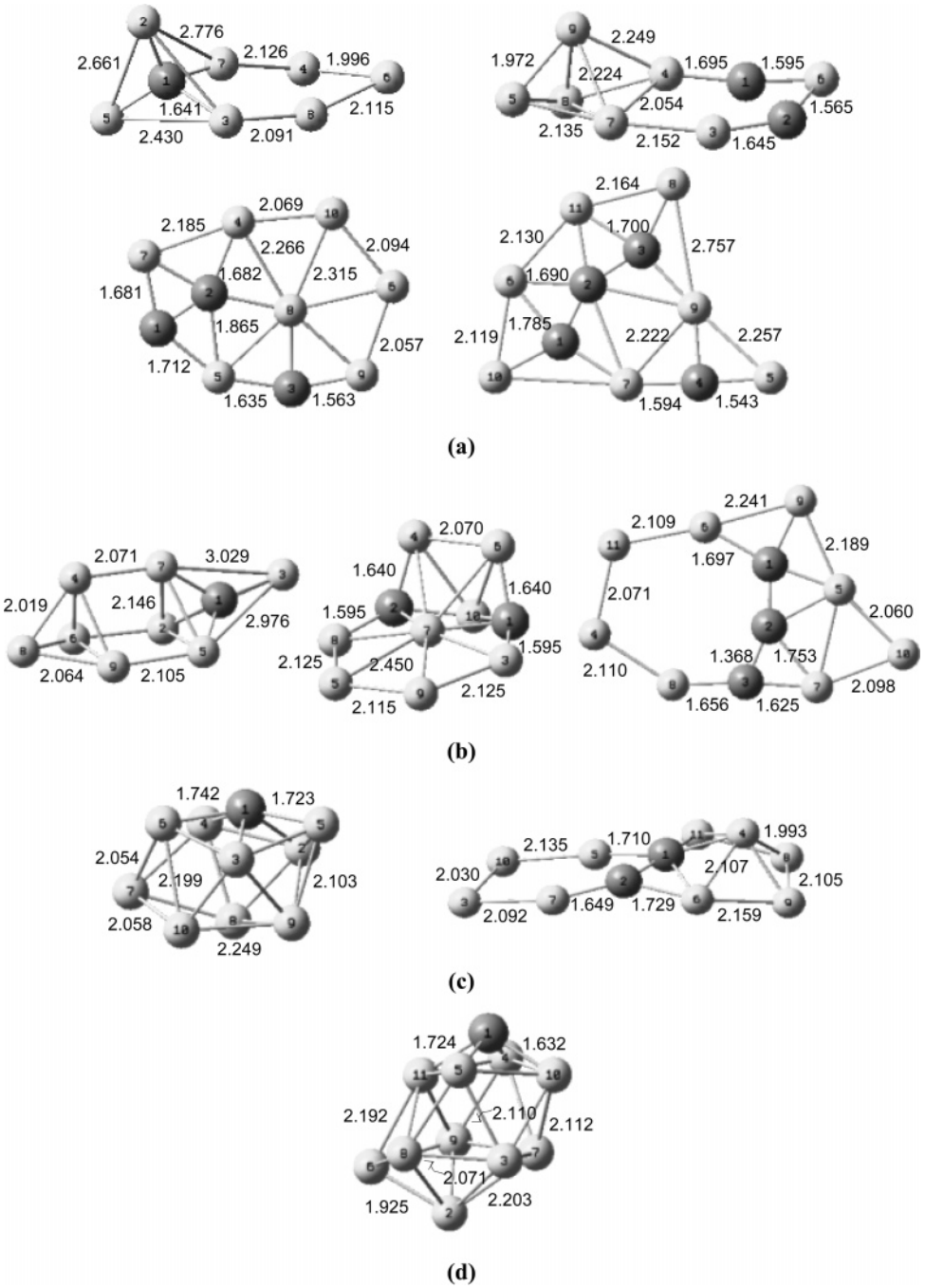

Figure 4. Same as Figure 1 for (a) Be_7C_m ($m = 1-4$), (b) Be_8C_m ($m = 1-3$), (c) Be_9C_m ($m = 1-2$), and (d) $Be_{10}C$ neutral clusters.

clusters are presented in the following sections and shown in Figures 1−4 along with selective bond lengths. Light and dark gray balls represent beryllium and carbon atoms respectively. Thirty-eight stable structures (not shown) with different spin multiplicity states but similar geometries as those of their corresponding ground state configurations are also discussed in this section.

3.1.1. $BeC_m(m = 1-10)$ Clusters. The ground state of the BeC dimer is a spin triplet ($C_{\infty v}$) with a bond length of 1.673 Å (Figure 1a). Two stable states of BeC, 0.20 and 1.79 eV less stable than the ground state, exist with higher (quintet) and lower (singlet) spin multiplicities and bond lengths of 1.639 and 1.674 Å, respectively. The BeC_m ($m = 2-7$) ground state clusters are all spin singlet and symmetric with respect to the Be-containing plane that is perpendicular to the cluster plane (Figure 1a). The ground state of BeC_2 is a spin singlet isosceles triangle (C_s) with both Be−C bond lengths of 1.612 Å and a C−C bond length of 1.275 Å (Figure 1a). A higher spin triplet multiplicity state, 2.44 eV less stable than the ground state, exists with elongated Be−C (by 0.019 Å) and C−C (by 0.081 Å) bond lengths.

The ground state of BeC_3 is a C_1 kite-shaped quadrilateral with Be−C and C−C bond lengths of 1.578 and 1.438 Å respectively, while BeC_4 is a symmetric irregular pentagon with symmetry C_1 (Figure 1a). A higher spin triplet multiplicity state, 1.66 eV less stable than the ground state, exists for BeC_4 with bond lengths elongated by 0.093 Å (Be−C) and 0.056 Å (first neighboring C−C, 1−2, and 3−4), and shortened by 0.076 Å (second neighboring C−C and 2−3) (Figure 1a).

The ground state of BeC_5 is an irregular hexagon with C_s symmetry. A higher spin triplet multiplicity state, 0.43 eV less stable than the ground state, exists with shortened Be−C (0.012

TABLE 1: Minimum and Maximum C−Be Bond Lengths and the Averages of All Minima and Maxima C−Be Bond Lengths in *n* Beryllium-Containing Be_nC_m ($n = 1-10$; $m = 1, 2, ...,$ to $11 - n$) Ground State Clusters per *n* Value

	C−Be (Å)			
n	minimum	maximum	average minimum	average maximum
1	1.564	1.753	1.64 ± 0.06	1.65 ± 0.06
2	1.570	1.700	1.64 ± 0.02	1.66 ± 0.02
3	1.526	1.677	1.62 ± 0.04	1.63 ± 0.04
4	1.538	1.874	1.60 ± 0.04	1.71 ± 0.10
5	1.566	1.901	1.62 ± 0.04	1.73 ± 0.08
6	1.520	1.895	1.56 ± 0.04	1.70 ± 0.12
7	1.543	1.865	1.57 ± 0.04	1.73 ± 0.10
8	1.589	1.803	1.60 ± 0.02	1.76 ± 0.06
9	1.649	1.824	1.67 ± 0.02	1.81 ± 0.02

Å) and elongated first and second neighboring C−C (0.088 and 0.014 Å) bond lengths, respectively. The ground state of BeC_6 is an irregular heptagon of C_s symmetry (Figure 1a). A higher spin triplet multiplicity state, 1.29 eV less stable than the ground state, exists with elongated Be−C, first neighboring C−C (2−3 = 1−6) and third neighboring C−C (4−5) bond lengths by 0.027, 0.017, and 0.128 Å, respectively, and shortened second neighboring C−C (3−4 = 5−6) bond lengths by 0.003 Å. The calculated ground state for BeC_7 is an irregular octagon of C_1 symmetry. A higher spin triplet multiplicity state, 0.35 eV less stable than the ground state, exists with shortened Be−C, first (1−2 = 6−7), second (2−3 = 5−6), and third (3−4 = 4−5) neighboring C−C bond lengths by 0.007, 0.005, 0.013, and 0.003 Å, respectively.

Ground states BeC_8 and BeC_9 are spin singlet and triplet with nonsymmetric irregular nonagon and decagon C_1 geometries, respectively (Figure 1a). A higher spin triplet multiplicity state for BeC_8, 0.98 eV less stable than the ground state, exists with Be−C bond lengths of 1.656 Å and C−C bond lengths of 1.254 Å (7−8, shortest) and 1.363 Å (1−8, longest), respectively. Two stable states of BeC_9, 0.13 and 0.68 eV less stable than the ground state, exist with lower (singlet) and higher (quintet) spin multiplicities and have Be10−C3 = 1.701 and 1.689, Be10−C9 = 1.698 and 1.663, and the shortest C−C (8−9 = 1.278 and 1.275 Å) and longest C−C (4−7 = 1.430 and 1.416 Å) bond lengths, respectively. The ground state for BeC_{10} is a spin singlet and shows a 3-D C_1 conformation (Figure 1a).

3.1.2. Be_2C_m($m = 1-9$) Clusters. The ground state of the Be_2C cluster is found to be a spin triplet isosceles triangle (C_s) with both the Be−C bond lengths of 1.631 Å and the Be−Be bond length of 2.132 Å (Figure 1b). Two stable states of Be_2C, 0.16 and 2.93 eV less stable than the ground state, exist with lower (singlet) and higher (quintet) spin multiplicities and have Be−C = 1.570 and 1.800 Å and Be−Be = 2.090 and 1.924 Å bond lengths, respectively.

It is interesting to notice that the ground states for Be_2C_2 (C_s) and Be_2C_3 (C_1) are almost linear spin triplet Be−C−C−Be and spin quintet Be−C−C−C−Be geometries, respectively, with both beryllium atoms at the extreme ends of the linear chains (Figure 1b), such as in the case of C−N chains where stable geometries correspond to linear carbon chains with the nitrogen atoms at the terminal positions.[46] A stable state of Be_2C_2, 3.33 eV less stable than the ground state, exists with quintet spin multiplicity and Be−C and C−C bond lengths of 1.642 and 1.330 Å, respectively. The ground state of Be_2C_4 is a spin singlet irregular C_s hexagon with Be−Be = 2.075 Å, Be−C = 1.686 Å, and Be−C neighboring C−C bond lengths of 1.255 (first) and 1.388 Å (second), respectively (Figure 1b).

The ground states of Be_2C_m ($m = 5-8$) show all planar C_1 cyclic structures where the two beryllium atoms are separated by two carbon atoms at one side and $m - 2$ carbon atoms at the other side. The Be_2C_m clusters with odd m are spin triplet, and the ones with even m are spin singlet. A stable state of Be_2C_5, 0.47 eV less stable than the ground state, exists with singlet spin multiplicity. In this isomer, the shortest (5−7) and longest (3−2) Be−C bond lengths are 1.650 and 1.700 Å, and the shortest (6−7) and longest (2−4) C−C bond lengths are 1.256 and 1.304 Å, respectively. A spin triplet state of Be_2C_6 that is 2.76 eV less stable than the ground state is observed. In that isomer, the shortest (5−7) and longest (6−1) Be−C bond lengths are 1.639 and 1.710 Å, and the shortest (8−7) and longest (1−4) C−C bond lengths are 1.250 and 1.330 Å, respectively (Figure 1b). A stable state of the Be_2C_7 cluster, 0.14 eV less stable than the ground state, exists with singlet spin multiplicity and with the shortest (9−8) and longest (6−3) Be−C bond lengths of 1.630 and 1.663 Å and the shortest (8−7) and longest (1−5) C−C bond lengths of 1.240 and 1.340 Å, respectively.

The ground state of Be_2C_9 is a spin triplet 3-D C_1 structure (Figure 1b). Two stable states of this cluster, 0.02 and 1.68 eV less stable than the ground state, exist with singlet and quintet spin multiplicities and bond lengths of Be11−C1 = 1.680 and 1.660 Å, Be10−C8 = 1.577 and 1.570 Å, C7−C5 = 1.417 and 1.500 Å, and C4−C3 = 1.256 and 1.260 Å, respectively (Figure 1b).

3.1.3. Be_3C_m($m = 1-8$) Clusters. The calculated ground state geometries of these clusters are all planar cyclic structures (Figure 2a). Be_3C is a spin triplet C_s kite-shaped quadrilateral with Be−C and Be−Be bond lengths of 1.581 and 2.103 Å, respectively. The ground state of the Be_3C_2 cluster is a spin singlet irregular pentagon of symmetry C_1. A stable state of this cluster, 0.34 eV less stable than the ground state, exists with triplet spin multiplicity and bond lengths of Be4−Be3 = 2.177 Å, Be5−Be3 = 2.120 Å, Be4−C1 = 1.660 Å, Be5−C2 = 1.650 Å, and C1−C2 = 1.260 Å. The ground state of Be_3C_3 is a spin singlet C_1 hexagon where the three Be atoms line up together separated by an average distance of 2.082 Å (Figure 2a).

The ground states of Be_3C_m ($m = 4-8$) are spin triplet for even m and spin singlet for odd m. These clusters show planar cyclic ring-type structures where there are always two sets of two beryllium atoms that are separated by two carbons, and the third set of beryllium atoms is separated by $m - 4$ carbon atoms. For instance, the ground state of the Be_3C_5 shows (Figure 2a) shows that atoms C1 and C2 are between the two beryllium atoms Be3 and Be8 (first Be set). Two other carbon atoms, C4 and C5, are placed between the atoms Be3 and Be7 (second Be set). This leaves only one carbon atom, C6, between the beryllium atoms Be8 and Be7 (third Be set). A similar effect has been observed before for Be_2C_m ($m = 5-8$) clusters where the two beryllium atoms are separated by two carbons at one side and $m - 2$ at the other side (Figure 1b).

The ground states of Be_3C_m ($m = 4-7$) and Be_3C_8 show symmetries C_1 and C_s, respectively (Figure 2a). A stable state of Be_3C_5, 1.28 eV less stable than the ground state, exists with singlet spin multiplicity and with the shortest (8−6) and longest (7−5) Be−C bond lengths of 1.630 and 1.640 Å and C−C bond lengths of 1.250 Å. A stable state of Be_3C_6, 2.92 eV less stable than the ground state, exists with triplet spin multiplicity and with the shortest (9−2) and longest (8−5) Be−C bond lengths of 1.640 and 1.770 Å and the shortest (4−6) and longest (1−2) C−C bond lengths of 1.250 and 1.310 Å, respectively (Figure 2a). A stable state of Be_3C_7, 0.75 eV less stable than the ground state, exists with singlet spin multiplicity and with the shortest

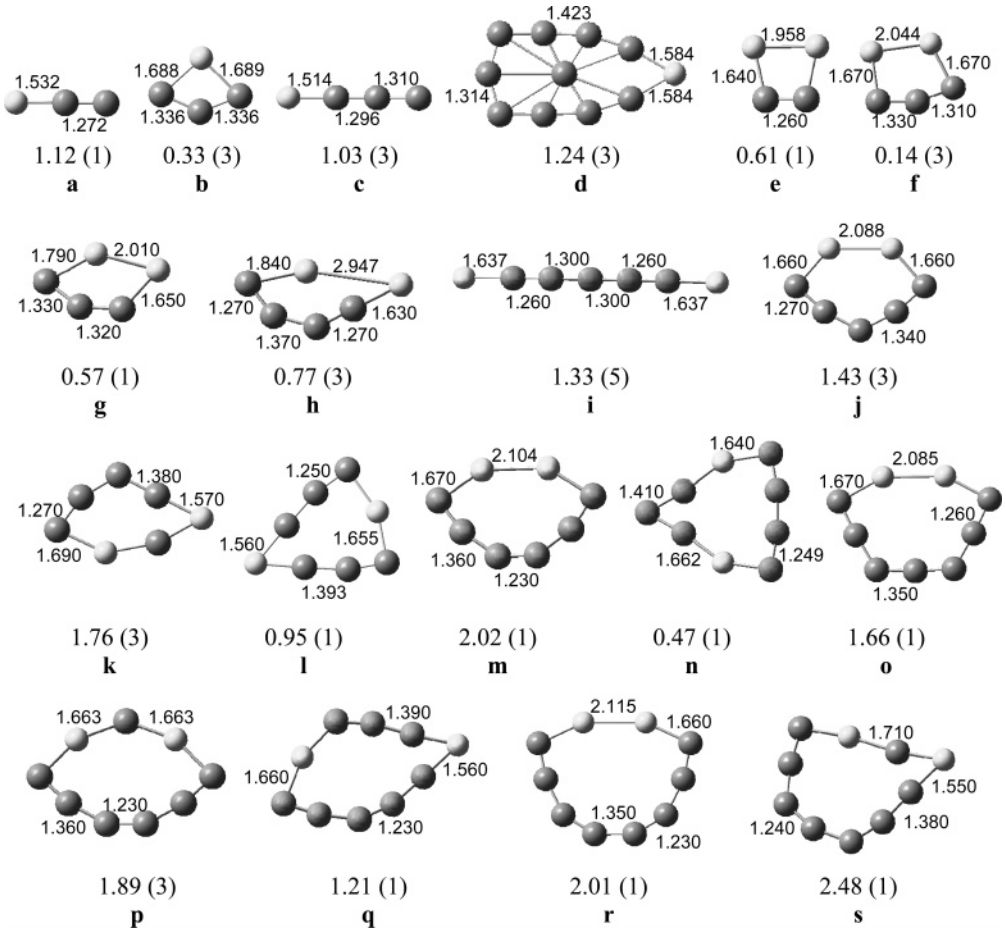

Figure 5. Stable isomers of BeC_m, $m = 2$ (a), 3 (b and c), and 10 (d) and Be_2C_m, $m = 2$ (e), 3 (f and g), 4 (h), 5 (i−k), 6 (l and m), 7 (n−p), and 8 (q−s) neutral clusters. Largest and smallest bond lengths per type of bond are in angstroms, relative energies with respect to their corresponding ground states are in electronvolts, and spin multiplicities (in parentheses) are reported. Light and dark gray balls represent beryllium and carbon atoms, respectively.

(5−3) and longest (7−2) Be−C bond lengths of 1.620 and 1.670 Å and the shortest (4−5) and longest (1−2) C−C bond lengths of 1.240 and 1.311 Å, respectively.

3.1.4. Be_4C_m ($m = 1-7$) Clusters. The ground state of a Be_4C cluster is a spin quintet C_s square of 2.250 Å sides with the beryllium atoms on its vertices and the carbon atom at the intersection of the diagonals (Figure 2b). The remaining ground states of Be_4C_m ($m = 2-7$) clusters are all spin singlet. Be_4C_2 shows symmetry C_s while Be_4C_3 and Be_4C_5 clusters show 3-D C_1 conformations, where the aforementioned pattern of having two carbon atoms between beryllium atoms in Be_2C_m ($m = 5-8$) and Be_3C_m ($m = 4-8$) ground states is also observed. In this particular cluster, however, the distribution of C and Be atoms is done in such a way that the "isolated" carbon atoms (C4 in Be_4C_3 and C5 in Be_4C_5) are the vertices of a tetrahedral beryllium agglomeration (Figure 2b). Be_4C_4 (C_1) and Be_4C_6 (C_1) clusters show planar cyclic conformations where the two-carbon atom pattern behavior is also observed. A stable state of the Be_4C_4 cluster, 1.52 eV less stable than the ground state, exists with triplet spin multiplicity and with both Be−Be bond lengths of 2.129 Å, Be4−C5 = 1.680 Å, Be6−C8 = 1.630 Å, and C−C= 1.270 Å. A stable state of the Be_4C_6 cluster, 0.25 eV less stable than the ground state, exists with triplet spin multiplicity and with the shortest (6−4) and longest (1−7) Be−C bond lengths of 1.650 and 1.730 Å and the shortest (8−9) and longest (3−2) C−C bond lengths of 1.240 and 1.260 Å, respectively. The ground state of Be_4C_7 is a spin singlet with a distorted ring C_s structure, having a Be atom in the center of the ring (Figure 2b).

3.1.5. Be_5C_m ($m = 1-6$) Clusters. The ground state of the Be_5C cluster is a spin singlet irregular pentagonal pyramid of symmetry C_1 (Figure 3a). Be_5C_2 is an irregular planar cyclic structure of symmetry C_1. A stable state of this cluster, 0.11 eV less stable than the ground state, exists with triplet spin multiplicity and bond lengths of Be3−Be6 = 1.910 Å, Be4−Be5 = 2.110 Å, Be1−C2 = 1.680 Å, and Be3−C7 = 1.670 Å. The Be_5C_3 ground state cluster is a 3-D C_1 irregular octagon where the carbon and beryllium atoms cluster separately (Figure 3a). The calculated Be_5C_4 (C_1), Be_5C_5 (C_1), and Be_5C_6 (C_s) ground state clusters are all planar systems with spin singlet multiplicity states. A stable state of Be_5C_4 cluster, 0.10 eV less stable than the ground state, exists with triplet spin multiplicity and bond lengths of Be5−Be9 = 2.110 Å, Be8−C1 = 1.860 Å, and Be7−C2 = 1.570 Å. The Be_5C_6 system perfectly follows the typical C−Be aforementioned pattern with all three pairs of carbon atoms distributed evenly between the Be atoms (Figure 3a).

3.1.6. Be_6C_m ($m = 1-5$) Clusters. The ground state of Be_6C is a spin triplet planar C_s distorted ring structure (Figure 3b). A stable state of this cluster, 0.42 eV less stable than the ground state, exists with singlet spin multiplicity and with the shortest (7−3) and longest (2−3) Be−Be bond lengths of 1.998 and 2.377 Å and the shortest (6−1) and longest (2−1) Be−C bond lengths of 1.547 and 1.629 Å, respectively. The ground states

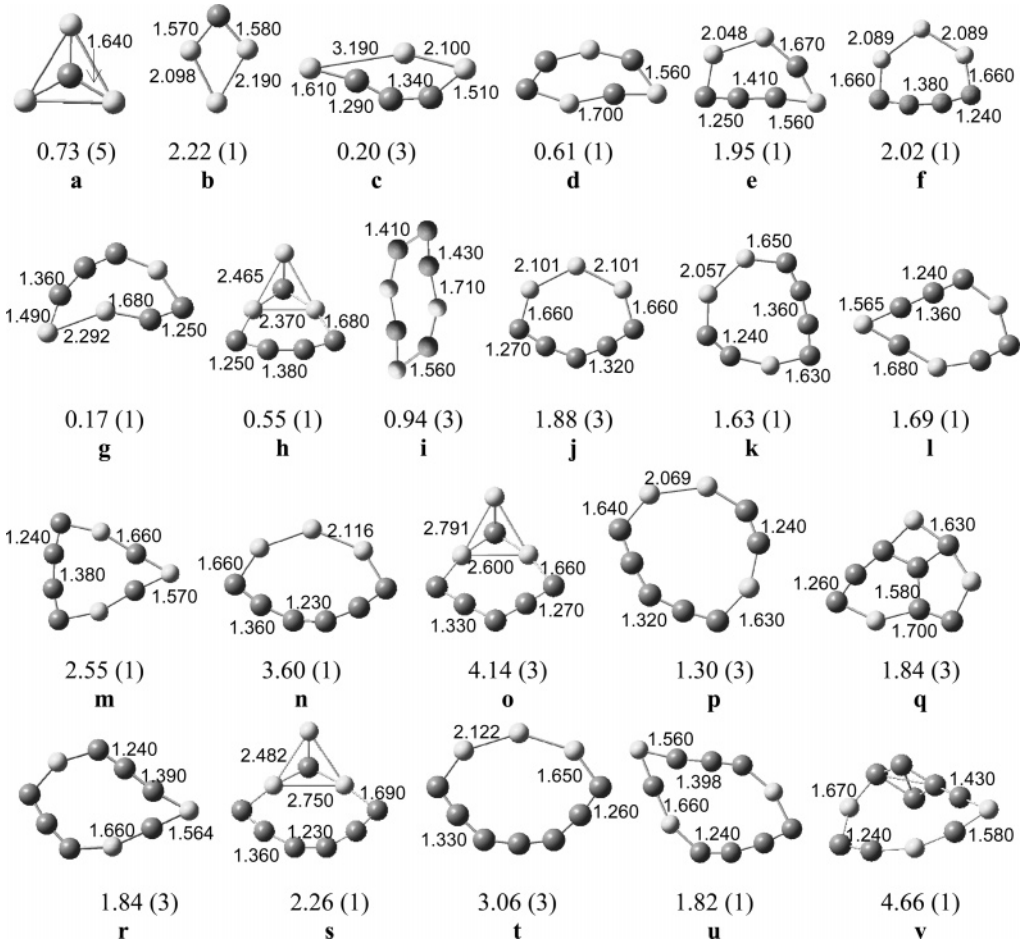

Figure 6. Same as Figure 5 for Be_3C_m, $m = 1$ (a and b), 3 (c), 4 (d−f), 5 (g−j), 6 (k−o), 7 (p−t), and 8 (u and v) neutral clusters.

of Be_6C_2 (C_1) and the Be_6C_3 (C_1) clusters are spin singlet and triplet planar structures, respectively (Figure 3b). Two stable states of the Be_6C_3 cluster, 0.10 and 0.19 eV less stable than the ground state, exist with higher (quintet) and lower (singlet) spin multiplicities and bond lengths of Be7−Be3 = 2.381 and 2.590 Å, Be4−Be9 = 2.071 and 2.079 Å, Be6−C2 = 1.606 and 1.615 Å, and Be5−C1 = 1.935 and 1.598 Å. Be_6C_4 and Be_6C_5 are three-dimensional C_1 systems with the Be_6C_5 structure perfectly antisymmetric along the axis containing the C2, C3, and C4 carbon atoms (Figure 3b), showing a "chair"-type structure. A stable state of Be_6C_5 cluster, 0.06 eV less stable than the ground state, exists with triplet spin multiplicity and bond lengths of Be7−Be9 = 2.575 Å and Be−C of 1.564 (7−1) and 1.735 (8−2) Å, respectively.

3.1.7. Be_7C_m ($m = 1-4$) Clusters. The ground states of Be_7C (C_1) and Be_7C_2 (C_1) clusters are three-dimensional quintet and singlet structures, respectively (Figure 4a). The Be_7C ground state has a pentagonal base and two beryllium atoms arranged in such a way that one is above this planar base and the other is below the base. A stable state of the Be_7C cluster, 0.96 eV less stable than the ground state, exists with septet spin multiplicity and with the shortest (4−6) and longest (3−5) Be−Be bond lengths of 1.972 and 2.776 Å and the shortest (5−1) and longest (7−1) Be−C bond lengths of 1.566 and 1.676 Å, respectively. A stable state of the Be_7C_2 cluster, 0.19 eV less stable than the ground state, exists with triplet spin multiplicity and the shortest (8−9) and longest (4−9) Be−Be bond lengths of 1.949 and 2.161 Å and the shortest (6−2) and longest (4−1) Be−C bond lengths of 1.566 and 1.707 Å, respectively.

The Be_7C_3 and Be_7C_4 ground states are both spin triplet planar C_1 systems (Figure 4a). Two stable states of the Be_7C_3 cluster, 0.13 and 1.04 eV less stable than the ground state, exist with lower (singlet) and higher (quintet) spin multiplicities and with the shortest (9−6) and longest (9−10) Be−Be bond lengths of 2.079 and 2.042 Å and 2.385 and 2.231 Å, respectively, the shortest (9−3) and longest (5−2) Be−C bond lengths of 1.590 and 1.575 Å and 1.937 and 1.839 Å, respectively, and C1−C2 = 1.937 and 1.379 Å. Two stable states of the Be_7C_4 cluster, 0.30 and 0.52 eV less stable than the ground state, exist with higher (quintet) and lower (singlet) spin multiplicities and Be−Be bond lengths of 2.683 and 2.956 Å (8−9) and 2.235 and 2.202 Å (7−9), Be−C bond lengths of 1.731 and 1.678 Å (7−1) and 1.579 and 1.524 Å (5−4), and C−C bond lengths of 1.390 and 1.400 Å (1−2) and 1.386 and 1.402 Å (2−3), respectively (Figure 4a).

3.1.8. Be_8C_m ($m = 1-3$), Be_9C_m ($m = 1-2$), and $Be_{10}C$ Clusters. Be_8C and Be_8C_2 are 3-D C_1 structures and Be_8C_3 is a C_1 planar system with spin multiplicities of five, one, and three, respectively (Figure 4b). A stable state of the Be_8C_2 cluster, 0.04 eV less stable than the ground state, exists with triplet spin multiplicity and bond lengths of Be4−Be6 = 2.071 Å, Be7−Be5 = 2.391 Å, Be7−C2 = 1.830 Å, and Be3−C1 = 1.587 Å. A stable state of the Be_8C_3 cluster, 0.45 eV less stable than the ground state, exists with singlet spin multiplicity and bond lengths of Be5−Be9 = 1.913 Å, Be7−Be10 = 2.041 Å, Be5−C2 = 1.770 Å, Be9−C1 = 1.586 Å, C1−C2 = 1.441 Å, and C2−C3 = 1.362 Å (Figure 4b). The ground state of the Be_9C (C_1) system is a spin triplet decagon with Be−Be bond lengths in the 2.05−2.25 Å range and C−Be bond lengths of ∼1.743 Å (Figure 4c). The ground state of Be_9C_2 (C_1) is also a 3-D spin triplet system with Be−Be in the 1.99−2.14 Å range and C−Be bond lengths in the 1.65−1.73 Å range. The ground state

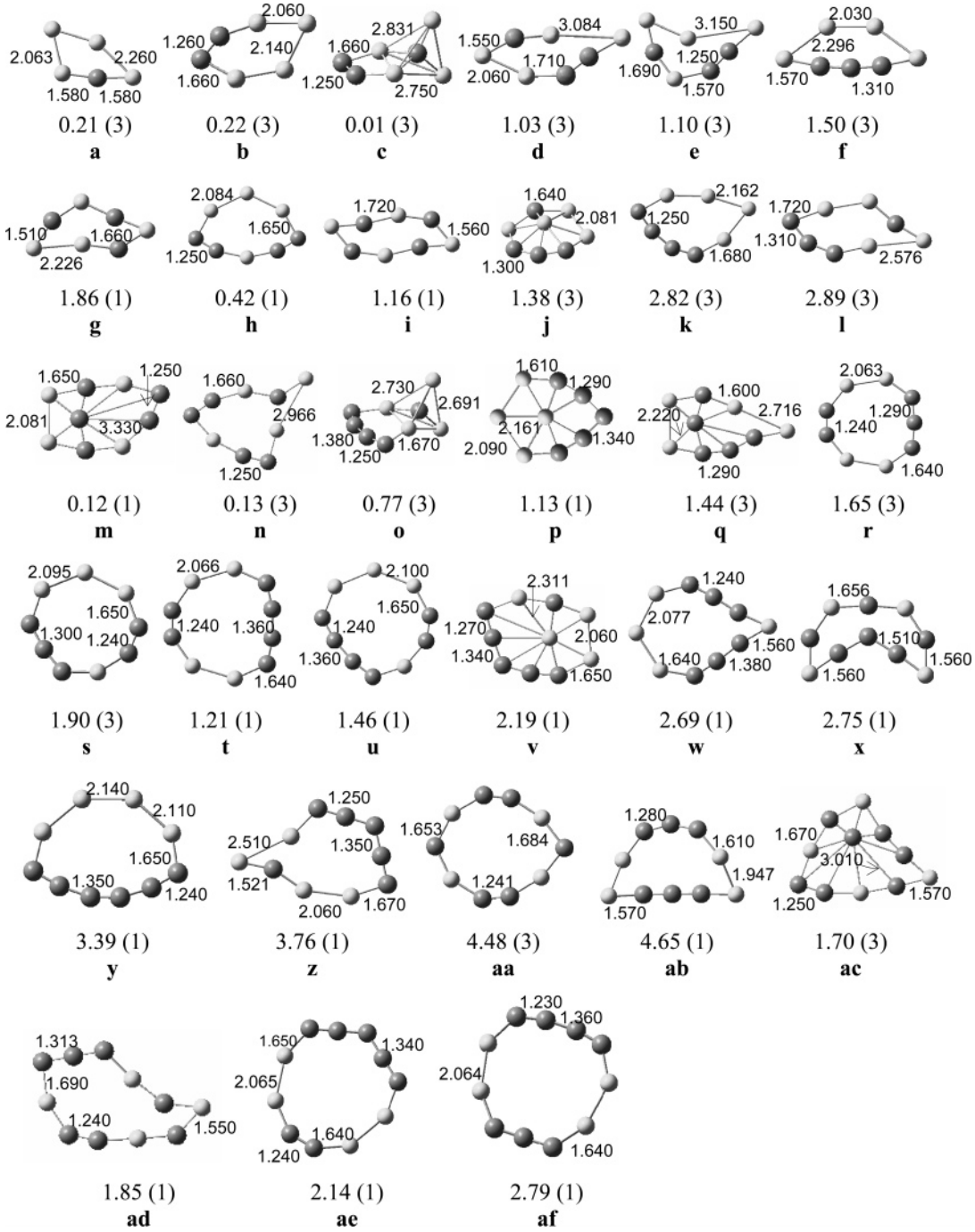

Figure 7. Same as Figure 5 for Be_4C_m, $m = 1$ (a), 2 (b), 3 (c−g), 4 (h−l), 5 (m−s), 6 (t−ab), and 7 (ac−af) neutral clusters.

geometry of $Be_{10}C$ (C_1) is a spin singlet undecagon with Be−Be in the 1.93−2.20 Å range and C−Be bond lengths in the 1.63−1.74 Å range (Figure 4d).

Overall, in all of the Be_nC_m $n = 1-10$, $m = 1, 2, ...,$ to $11 - n$ ground state clusters, the Be−Be, first neighboring C−C, second neighboring C−C, and Be−C bond lengths are in the 2.04−2.26, 1.24−1.44, 1.29−1.38, and 1.52−1.90 Å ranges, respectively. As far as we are aware, there are no published experimental data for the bond lengths of Be−C neutral clusters, except for the "typical" reported C−Be bond length of 1.93 Å.[85] In Table 1 the minimum and the maximum C−Be bond lengths and the average of all minima and maxima C−Be bond lengths in n beryllium-containing Be_nC_m ($n = 1-10$; $m = 1, 2, ...,$ to $11 - n$) ground state clusters are reported per n value. The standard deviation is calculated using the "nonbiased" or "$n - 1$" method to estimate errors in computing averages (±2 deviations of the mean).[86] The maximum of all C−Be bond lengths observed in this small cluster corresponds to 1.901 Å for the case of $n = 5$. The average of all maxima C−Be bond lengths in n-beryllium-containing clusters shows a clear increase with n, from 1.65 ± 0.06 Å for $n = 1$ to 1.81 ± 0.02 Å for $n = 9$, getting closer to the typical bond length of 1.93 Å.[85]

3.2. Higher-Energy Isomers. Isomers of Be_nC_m ($n = 1-10$; $m = 1, 2, ...,$ to $11 - n$) have the same chemical formula (composition) but different conformations and/or atomic arrangements than those of their ground state counterparts and therefore exhibit different chemical and physical properties than the ground states. Hence, in this section, 113 isomers of ground state conformations (Figures 1−4) found at the B3PW91/6-31+G* DFT theory level are presented and briefly discussed.

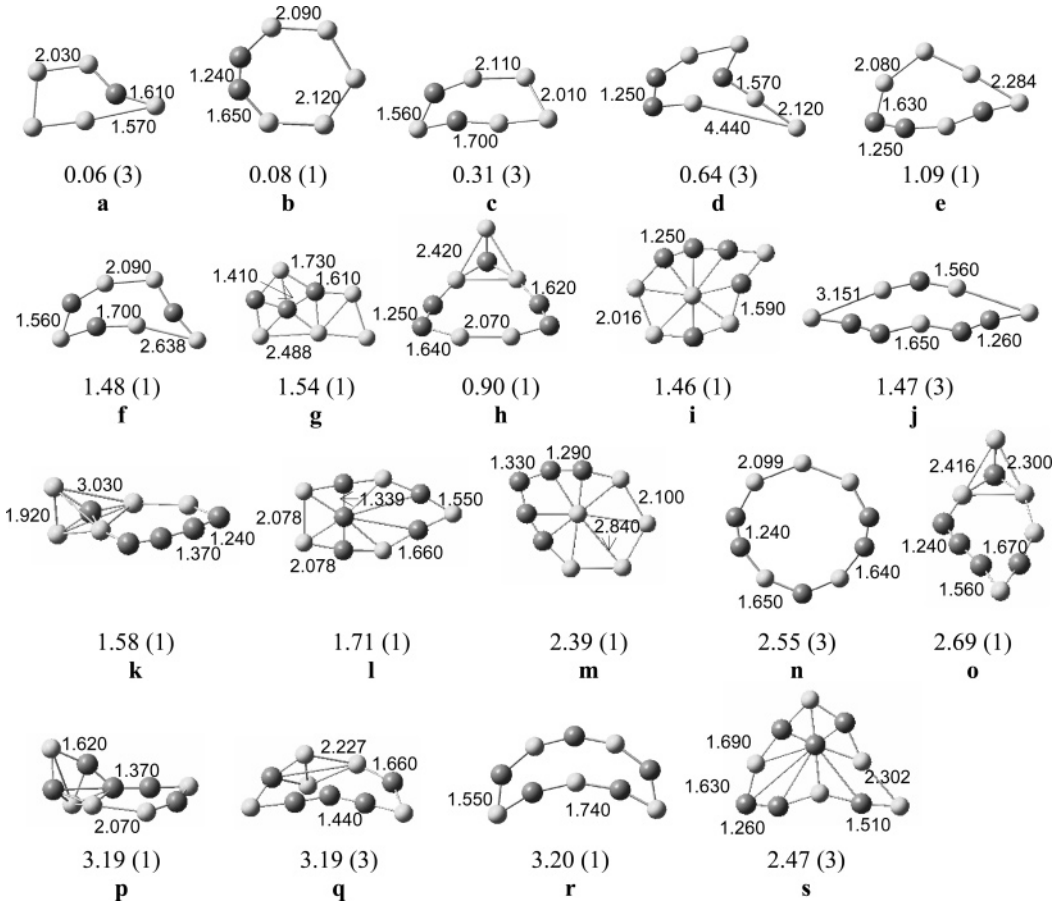

Figure 8. Same as Figure 5 for Be_5C_m, $m = 1$ (a), 2 (b and c), 3 (d−g), 5 (h−r), and 6 (s) neutral clusters.

Particular attention is given to planar cyclic isomers showing different arrangement of the *n* beryllium and *m* carbon atoms. Figures 5−9 summarize isomer geometries along with the shortest and longest bond lengths per type of bond (Be−Be, Be−C, or C−C), relative energies with respect to their corresponding ground states, and spin multiplicities (in parentheses). Light and dark gray balls represent beryllium and carbon atoms, respectively.

From all of the possible arrangements in which Be and C atoms can combine to form Be_2C_m ($m = 5-8$) clusters, the pattern of having the beryllium atoms separated by two carbon atoms at one side and $m - 2$ carbon atoms at the other side of the Be atoms is the most stable (ground states, Figure 1b), followed by clusters where the two Be atoms are separated by three carbon atoms at one side and $m - 3$ ($m = 7$ and 8) carbon atoms at the other side of the Be atoms (Figures 5n and 5q). Next, for Be_2C_m ($m = 5$, 7, and 8), clusters where the Be atoms are together, i.e., separated by 0 carbon atoms on one side and *m* on the other side (Figures 5j, 5o, and 5r), and finally clusters where the two Be atoms are separated by one carbon atom at one side and $m - 1$ at the other side (Figures 5k, 5p, and 5s). Only two isomers are found in the case of Be_2C_6 at the B3PW91/6-31+G* theory level. The first one has the two Be atoms separated by one carbon atom at one side and $m - 1$ (= 5) at the other side, and the least stable one has the Be atoms together (Figures 5l and 5m).

The most stable geometries of Be_3C_m ($m = 4-8$) clusters (ground states, Figure 2a) always show two sets of two beryllium atoms that are separated by two carbons, and the third set of beryllium atoms separated by $m - 4$ carbon atoms. Energetically this type of arrangement is followed by the stable planar cyclic isomers of Be_3C_m ($m = 4-7$) clusters (Figures 6d, 6g, 6k, and 6p), where the clusters have one set of two carbon atoms separating two beryllium atoms, followed by isomers where three Be atoms have one and three carbon atoms between them, respectively (Figures 6e, 6i, 6l, and 6r), and the least stable configuration is the one where all three Be atoms cluster together (Figures 6f, 6j, 6n, and 6t). In the case of the planar isomer of Be_3C_8 (Figure 6u), the geometry of having one set of two carbon atoms separating two beryllium atoms is not found at the B3PW91/6-31+G* theory level. However, the observed most stable isomer configuration follows the aforementioned trend, in which three Be atoms have one and three carbon atoms between them, respectively (Figure 6u).

Three-dimensional isomers are also observed for Be_3C_m ($m = 5-8$) clusters. It is interesting to discuss a particular 3-D structure consistently observed for $m = 5-7$. These geometries have a planar base structure where two Be atoms are separated by one C atom at one side and $m - 1$ C atoms, respectively, at the other side, and one Be atom is out of the plane, forming a beryllium tetrahedron centered on the isolated C atom (Figures 6h, 6o, and 6s).

The most stable geometry of planar cyclic Be_4C_m (even *m*) clusters (ground states, Figure 2b) always shows at least one set of two beryllium atoms that are separated by two carbon atoms. The following stable planar cyclic isomers of Be_4C_m ($m = 5-7$) clusters have at least one set of two carbon atoms separating two beryllium atoms (Figures 7n, 7t, and 7ad), followed by isomers where the four Be atoms have 0, 2, 0, and $m - 2$ C atoms between them as we move around the cycle (Figures 7r, 7u, and 7ae) and then by a configuration where the four Be atoms are separated by 0, 0, 3, and $m - 3$ C atoms as

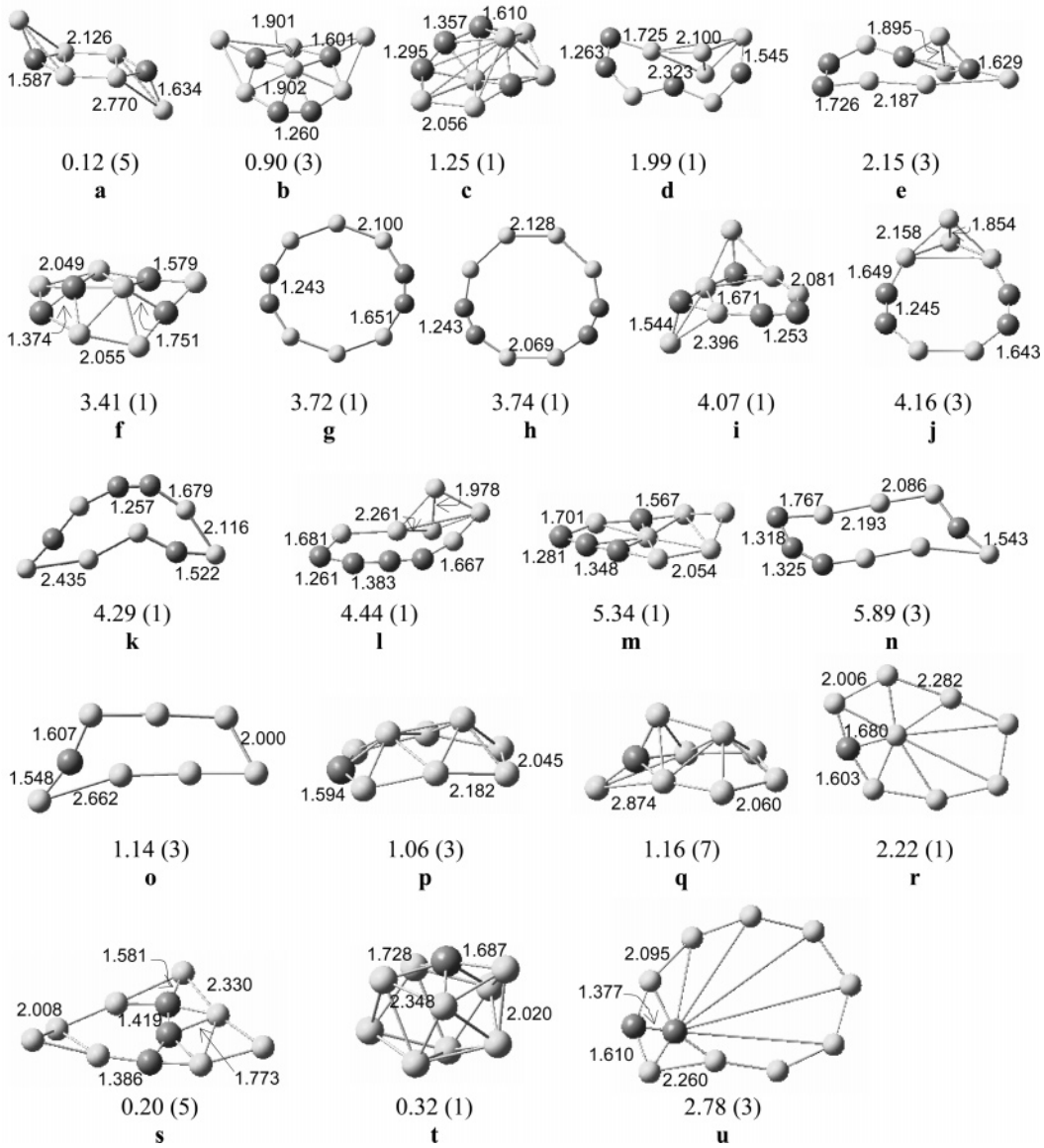

Figure 9. Same as Figure 5 for Be_6C_m, $m = 2$ (a) and 4 (b−n), Be_7C (o), Be_8C_m, $m = 1$ (p−r) and 3 (s), and Be_9C_m, $m = 1$ (t) and 2 (u) neutral clusters.

we move around the cycle (Figures 7s and 7w) for $m = 5$ and 6. The latter conformation is not seen at the theory level of this work for Be_4C_m; instead the least energetic geometry observed shows the four Be atoms having 0, 3, 0, and $m - 3$ C atoms as we move around the cycle (Figure 7af). As the number of beryllium atoms in the cluster (n) increases, less clear trends on atomic arrangement can be drawn. However, the most stable planar cyclic higher-energy isomers of Be_5C_m ($m = 2$, 3, and 5) (Figures 8b, 8d, and 8j) and Be_6C_4 (Figure 9g) clusters have always at least a set of 2 C atoms in between two Be atoms.

3.3. Stability of Ground State Clusters. In this section, binding energies per atom, E_b, second differences in energies, $\Delta_2E(m)$, HOMO−LUMO gaps (HLGs), and vertical ionization potentials (IP_v's) and electron affinities (EA_v's) for ground state Be_nC_m ($n = 1-10$, $m = 1, 2, ...,$ to $11 - n$) clusters are presented and discussed. Table 2 summarizes the calculated values of E_b, HLG, IP_v, EA_v, and $\Delta_2E(m)/n$ for these clusters, which are ordered according to E_b from the most to the least stable for decreasing N ($= n + m$) value. All of these energy-related properties are then used for the identification of magic Be_nC_m clusters.

3.3.1. Binding Energy and Second Difference in Energy. The binding energy per atom for the neutral clusters is calculated according to

$$E_b = \frac{mE(C) + nE(Be) - E(Be_nC_m)}{N}$$

where E(C) is the energy of a single carbon atom, E(Be) is the energy of a single Be atom, $E(Be_nC_m)$ is the energy of the Be_nC_m cluster ($n = 1-10$, $m = 1, 2, ...,$ to $11 - n$), and N is the total number of atoms in the cluster ($N = n + m$).

The calculated binding energy per atom E_b is plotted as a function of the cluster size, N, in Figure 10a. It is interesting to notice that BeC_m ($m = 1-9$) shows the highest binding energy per atom for $2 \le N \le 9$ and $N = 11$, while Be_2C_8 shows a slightly higher binding energy per atom (5.34 eV) than BeC_9 (5.30 eV) for $N = 10$ (Table 2). Hence, it is reasonable to conclude that Be_nC_m clusters containing one Be atom seem to be the most stable ones. However, the lowest E_b value is always reached by the highest possible value of n in each Be_nC_m cluster (Figure 10a, Table 2). It is also observed that the clusters with odd numbers of beryllium atoms, n, (Figure 10a, filled symbols)

TABLE 2: Calculated $\Delta_2E(m)$, HOMO−LUMO Gap (HLG), IP_v, and EA_v for Be_nC_m ($n = 1-10$; $m = 1, 2, ...,$ to $11 - n$) Clusters[a]

N	n	m	E_b (eV)	HLG (eV)	IP_v (eV)	EA_v (eV)	$\Delta_2E(m)/n$ (eV)	N	n	m	E_b (eV)	HLG (eV)	IP_v (eV)	EA_v (eV)	$\Delta_2E(m)/n$ (eV)
11	1	10	**5.26**	3.04	6.84	3.47		8	1	7	**5.30**	2.49	8.22	3.66	−0.11
11	3	8	5.18	**4.72**	**8.01**	2.14		8	2	6	5.11	**5.14**	**9.46**	**2.04**	**1.17**
11	2	9	5.05	2.71	6.22	3.64		8	3	5	4.44	4.41	8.67	2.87	−1.21
11	4	7	4.54	2.58	5.98	2.63		8	4	4	4.02	3.49	8.10	2.51	0.10
11	5	6	4.33	3.48	6.94	**1.86**		8	5	3	3.39	1.92	6.05	2.48	0.47
11	6	5	3.73	1.19	5.34	3.40		8	6	2	2.54	1.15	5.82	3.41	−0.22
11	7	4	3.37	2.35	5.25	3.90		8	7	1	2.01	2.92	6.20	2.15	0.03
11	8	3	2.80	1.61	5.65	2.71		7	1	6	**5.17**	3.81	**8.95**	2.57	**2.80**
11	9	2	2.43	1.43	5.38	3.01		7	2	5	4.74	**4.50**	8.44	2.68	−0.36
11	10	1	2.40	2.03	5.76	2.65		7	3	4	4.32	3.98	8.47	**1.94**	**1.18**
10	2	8	**5.34**	4.17	**8.28**	2.72	**2.50**	7	4	3	3.60	2.88	6.91	1.96	0.24
10	1	9	5.30	2.93	7.15	3.74	−0.55	7	5	2	2.70	1.75	5.96	2.13	−0.33
10	3	7	4.94	**4.44**	7.55	2.80	−0.85	7	6	1	1.89	2.59	6.03	2.58	−0.19
10	4	6	4.58	2.81	6.80	2.78	0.75	6	1	5	**4.54**	3.04	8.38	2.68	−5.06
10	5	5	4.13	3.01	6.47	2.07	0.39	6	2	4	4.38	**3.63**	**8.46**	**1.81**	**0.31**
10	6	4	3.87	3.74	6.32	**1.31**	**1.27**	6	3	3	3.57	1.64	7.10	2.88	−0.97
10	7	3	3.01	2.14	5.81	3.22	−0.01	6	4	2	2.88	2.15	6.63	1.90	−0.29
10	8	2	2.71	1.52	5.77	2.91	0.52	6	5	1	2.05	1.76	6.48	2.29	−0.05
10	9	1	2.32	2.43	5.41	2.62	0.44	5	1	4	**4.66**	3.91	**9.73**	2.38	**3.38**
9	1	8	**5.41**	3.58	7.98	2.68	2.02	5	2	3	3.75	**5.54**	7.33	2.13	−1.40
9	2	7	5.13	3.91	7.54	3.37	−0.93	5	3	2	3.12	2.71	7.07	1.55	0.40
9	3	6	4.93	**5.13**	**8.95**	**2.03**	**1.30**	5	4	1	2.11	4.22	6.61	**1.04**	−0.20
9	4	5	4.30	2.73	7.90	3.48	−0.14	4	1	3	**4.00**	1.96	**8.09**	2.58	−2.36
9	5	4	3.67	2.47	6.09	2.64	−0.48	4	2	2	3.50	**6.26**	7.49	**1.13**	**1.97**
9	6	3	3.19	2.42	5.97	2.44	−0.26	4	3	1	2.13	2.99	6.89	2.33	−0.01
9	7	2	2.57	1.73	5.66	2.69	0.01	3	1	2	**3.68**	**3.39**	**9.35**	2.13	**3.59**
9	8	1	2.13	2.88	5.85	2.58	−0.12	3	2	1	1.77	3.04	7.43	**2.03**	−1.81
								2	1	1	1.24	2.86	9.60	0.44	−6.06

[a] Clusters are ordered according to $\Delta_2E(m)$ from the most (bold) to the least stable in terms of E_b for decreased N ($= n + m$) value.

show comparatively higher binding energies than the clusters containing even numbers of beryllium atoms (Figure 10a, empty symbols), which makes them relatively more stable.

In Figure 10a the minimum (dotted line) binding energy trend curve shows a clear change of behavior at $N = 7$, a value after which this curve increases almost linearly with N, possibly indicating an intrinsic change in the behavior of small BeC clusters. To elucidate this point, the relative stabilities of the clusters upon the addition or elimination of a carbon atom are calculated using the second difference of energy $\Delta_2E(m)$, which is calculated as

$$\Delta_2E(m) = E(Be_nC_{m-1}) + E(Be_nC_{m+1}) - 2E(Be_nC_m)$$

where $E(Be_nC_{m-1})$, $E(Be_nC_{m+1})$, and $E(Be_nC_m)$ are the energies of the n-beryllium Be_nC_{m-1}, Be_nC_{m+1}, and Be_nC_m clusters ($n = 1-10$, $m = 1, 2, ...,$ to $11 - n$), respectively. In cluster physics,[6,87] the second difference in energy can be used to search for "magic clusters". This quantity represents the relative stability of a pure cluster with respect to its two immediate neighbors and can be compared directly to the experimental abundance.[6] Because this study does not consider pure clusters, i.e., formed by only one type of element, two equations for the second difference in energy can be written, one at constant n, $\Delta_2E(m)$, and the other at constant m, $\Delta_2E(n)$. Both possibilities were explored, but $\Delta_2E(m)$ is presented here due to its clearer trends and ease to follow the organization of this paper.

The aforementioned equation for $\Delta_2E(m)$ can be rewritten as the sum of two differences, $[E(Be_nC_{m-1}) - E(Be_nC_m)] + [E(Be_nC_{m+1}) - E(Be_nC_m)]$. The first difference is the relative stability of Be_nC_m with respect to the addition of a carbon atom to the Be_nC_{m-1} cluster, and the second difference is the relative stability of Be_nC_m with respect to the elimination of a carbon atom from the Be_nC_{m+1} cluster. Hence, if Be_nC_m is indeed more stable than its neighbors, then both differences and therefore $\Delta_2E(m)$ are positive. To "normalize" $\Delta_2E(m)$ and get rid of relative comparisons between all ground state clusters, the quantity $\Delta_2E(m)/n$, where n is the number of Be atoms in the cluster, is considered instead. Hence, $\Delta_2E(m)/n$ provides a qualitative measure of absolute Be_nC_m cluster stability upon the addition and removal of one carbon atom to the clusters.

In Figure 10b the n value that gives the highest and the lowest $\Delta_2E(m)/n$ per each N is plotted as a function of N. According to this figure, it is evident that the highest $\Delta_2E(m)/n$ is always achieved by $n = 1$ for odd m and $n = 2$ for even m and that the lowest $\Delta_2E(m)/n$ is achieved by $n = 2$ for odd m in Be_nC_m, respectively, and irrespective of the cluster size N. When N is even and $N > 6$, however, a different behavior is observed because the lowest $\Delta_2E(m)/n$ values are obtained by $n = 3$. Hence, it is concluded that the highest Be_nC_m cluster stability with respect to the addition or removal of a carbon atom is achieved by BeC_m (odd m) and Be_2C_m (even m) irrespective of the total number of atoms in the cluster. Moreover, Be_2C_m (odd m), BeC_m ($m = 4$ and 6), and Be_3C_m (odd $m = 8$ and 10) clusters are the least stable with respect to the addition or removal of a carbon atom (Figure 10b). Thus, two different trends are observed from this figure for $N < 7$ and $N > 7$ with respect to the number of beryllium atoms that minimize $\Delta_2E(m)/n$ per each N, explaining the intrinsic change in the behavior of small BeC clusters at $N = 7$ in the minimum binding energy trend curve of Figure 10a.

Figures 11a and 11b show the behavior of $\Delta_2E(m)/n$ as a function of n for odd and even total numbers of atoms, $N = n + m$, in the Be_nC_m clusters, respectively. It can be noted that there is an even−odd alternation in these $\Delta_2E(m)/n$ values with n. This figure clearly shows that clusters with odd n and N (Figure 11a) and clusters with even n and N (Figure 11b) are particularly stable.

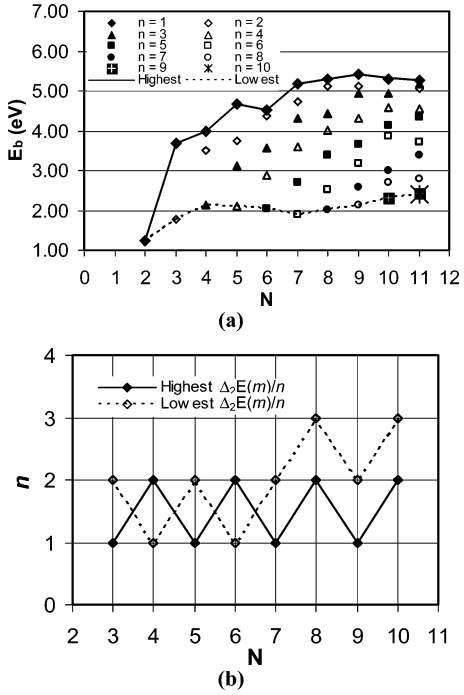

Figure 10. (a) Binding energy per atom as a function of the cluster size N ($= n + m$) for Be_nC_m ($n = 1-10$; $m = 1, 2, ...,$ to $11 - n$) clusters. (b) n vs N for the highest and lowest $\Delta_2E(m)/n$ according to Table 2.

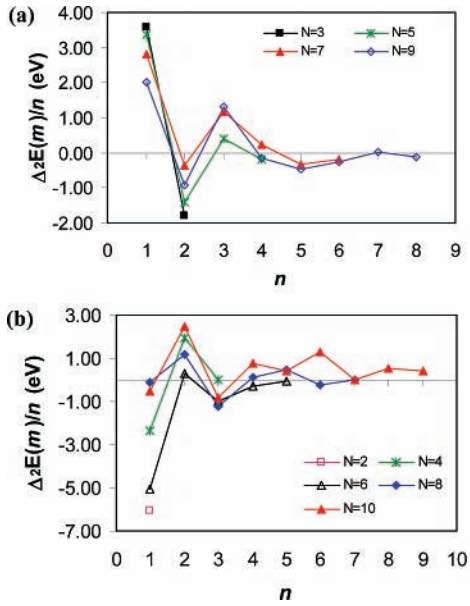

Figure 11. Second difference in energy per beryllium atom, $\Delta_2E(m)/n$, vs number of beryllium atoms, n, for odd (a) and even (b) total numbers of atoms in the cluster, $N = n + m$.

3.3.2. HOMO−LUMO Gap, Vertical Ionization Potential, and Electron Affinity. The HLG/ band gap is the energy difference between the highest occupied (HOMO) and the lowest unoccupied (LUMO) molecular orbitals. Figure 12 shows the variation of HLG as a function of the cluster size N. It is interesting to notice that the highest HLG is observed when $n = 1$, $n = 2$, and $n = 3$ for $N = 3$, 4−8, and 9−11, respectively. Similarly, the lowest HLG is observed when $n = 2$, 1, 3, 3, 5, 6, 7, 8, and 6 for $N = 3-11$, respectively. Overall, the highest and lowest HLGs are reached by Be_2C_2 and Be_6C_2, respectively (Figure 12).

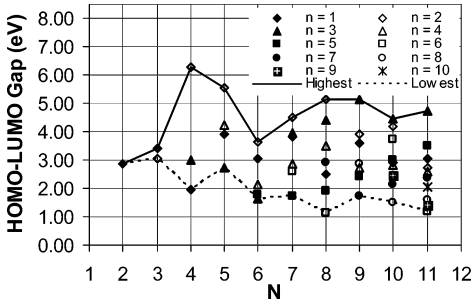

Figure 12. HOMO−LUMO gaps as a function of the number of atoms in the cluster ($N = n + m$) for Be_nC_m ($n = 1-10$; $m = 1, 2, ...,$ to $11 - n$) neutral clusters.

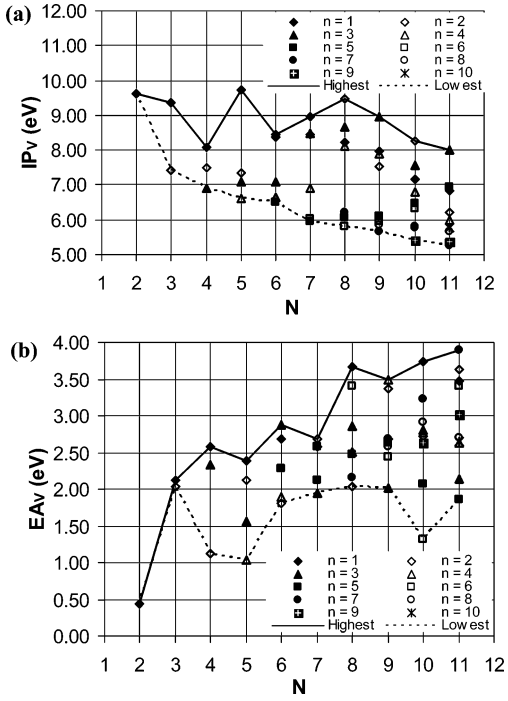

Figure 13. Vertical (a) ionization potential, IP_v, and (b) electron affinity, EA_v, as functions of N ($= n + m$) for all of the Be_nC_m ($n = 1-10$; $m = 1, 2, ...,$ to $11 - n$) neutral ground state clusters.

The ionization potential and the electron affinity are defined as the energy needed for the removal of an electron from the cluster and the energy released when an extra electron is added to the neutral atom, respectively, yielding valuable information on the electronic structure of the cluster.[5] The vertical ionization potential and vertical electron affinity are "first order" ionization potentials and electron affinities, respectively, and calculated using the following equations

$$IP_v = E[Be_nC_m]^+ - E[Be_nC_m]$$

$$EA_v = E[Be_nC_m] - E[Be_nC_m]^-$$

where $E[Be_nC_m]^+$ and $E[Be_nC_m]^-$ are the energies corresponding to singly positively and negatively charged clusters at the neutral cluster's geometry, respectively.

Figures 13a and 13b show the vertical ionization potential and vertical electron affinity as functions of the cluster size, respectively. The solid and dotted lines in Figures 13a and 13b join the highest and the lowest calculated IP_v and EA_v values for each N.

It is interesting to notice that IP_v is maximum at $n = 1$, $n = 2$, and $n = 3$ for $N = 3-5$, and 7, $N = 6$, 8, and 10, and $N =$

9 and 11, respectively. The IP_v minimum is found when $n = 2$, 3, 4, 5, 5, 6, 7, 9, and 7 for $N = 3-11$, respectively (Figure 13a). However, EA_v is maximum at $n = 1$, 1, 1, 3, 2, 1, 4, 1, and 7 for $N = 3-11$, and it is minimum when $n = 2$, 2, 4, 2, 3, 2, 3, 6, and 5 for $N = 3-11$, respectively.

3.3.3. Magic Numbers. The stability of Be_nC_m ($n = 1-10$; $m = 1, 2, ...,$ to $11 - n$) clusters can be discussed on the basis of E_b, HLG, IP_v, EA_v, and $\Delta_2E(m)/n$. In Table 2, E_b, HLG, IP_v, EA_v, and $\Delta_2E(m)/n$ of the Be_nC_m ground state structures shown in Figures 1−4 are reported, where clusters are ordered per each N from the most to the least stable (in terms of E_b) for decreased N. Hence, the most and least stable clusters correspond to the cases for which E_b are the highest and lowest, respectively, per N. In Table 2, the highest E_b, HLG, IP_v and lowest EA_v are in bold for clear visualization of clusters with particular stabilities. In addition, when a cluster has any of those quantities highlighted, $\Delta_2E(m)/n$ is also highlighted when positive. Note that for clusters containing a total of 11 atoms no value for $\Delta_2E(m)/n$ is reported because their calculations required information about clusters containing 12 atoms, which were not studied in this work.

Table 2 clearly shows that BeC_m ($m = 1-9$) clusters have the highest binding energy per atom for $2 \leq N \leq 9$ and $N = 11$, while Be_2C_8 shows a slightly higher binding energy per atom (5.34 eV) than BeC_9 (5.30 eV) for $N = 10$ as discussed previously. The most stable 5-, 7-, and 10-atom clusters are the ones that exhibit the highest E_b, IP_v, and $\Delta_2E(m)/n$. The most stable 4-atom cluster is the one that exhibits the highest E_b and IP_v. The most stable 6-, 8-, and 11-atom clusters are the ones that exhibit the highest E_b. The most stable 9-atom cluster is the one that exhibits the highest E_b and $\Delta_2E(m)/n$. Finally, the most stable 3-atom cluster is the one that exhibits the highest E_b, HLG, IP_v, and $\Delta_2E(m)/n$. No correlation has been found between EA_v and cluster stability.

According to Table 2, at particular values of n and m certain Be_nC_m clusters show particular stability and are expected to have higher abundances than their neighboring clusters. Clusters having two or more properties highlighted and a positive $\Delta_2E(m)/n$ in Table 2 are considered particularly stable. These clusters (Be_2C_8, Be_3C_6, Be_2C_6, BeC_6, Be_2C_4, BeC_4, Be_2C_2, and BeC_2) are then referred to as clusters of "magic numbers", indicating that the clusters with these values of n are more stable than their neighboring clusters. The particularly high stabilities of BeC_2, BeC_4, and BeC_6 can be understood in view of the magic numbers of total valence electrons of 10, 18, and 26, respectively. However, the particularly high stabilities of Be_2C_2, Be_2C_4, Be_2C_6, Be_2C_8, and Be_3C_6 clusters containing 12, 20, 28, 36, and 30 total valence electrons, respectively, may be due to atomic structure effects.

4. Conclusions

Studies on the structure and stability of Be_nC_m ($n = 1-10$; $m = 1, 2, ...,$ to $11 - n$) clusters have been conducted at the B3PW91/6-31+G* DFT level. The most stable planar cyclic conformations always show at least a set of two carbon atoms between two beryllium atoms, while structures where beryllium atoms cluster together, or allow the intercalation of one carbon atoms between two of them, generally seem to be the least stable ones. The stability of Be_nC_m ground clusters is discussed on the basis of their binding energy per atom, HOMO−LUMO gap, vertical ionization potential, vertical electron affinity, and second difference in energy per beryllium atom. Be_2C_8, Be_3C_6, Be_2C_6, BeC_6, Be_2C_4, BeC_4, Be_2C_2, and BeC_2 are identified as clusters of "magic numbers" and may be further considered in the assembly of more complex structures with unique properties for technological applications.

Acknowledgment. The support of the National Science Foundation (Grant No. NSF-DMR-0414903) that funded the SGI Altix3700 computational resource used for this study and the partial support of DARPA and Navy SPAWAR SC under Award No. 66001-05-1-8903 are gratefully acknowledged.

References and Notes

(1) Jena, P.; Behera, S. N. *Clusters and Nanostructured Materials*; Nova Science: New York, 1996.
(2) Kumar, V.; Esfarjani, K.; Kawazoe, Y. *Clusters and Nanomaterials*; Springer-Verlag: Berlin, 2002.
(3) Alonso, J. A. *Chem. Rev.* **2000**, *100*, 637.
(4) Alonso, J. A. *Structure and Properties of Atomic Nanoclusters*; Imperial College Press: London, 2006.
(5) De Heer, W. A. *Rev. Mod. Phys.* **1993**, *65*, 611.
(6) De Heer, W. A.; Knight, W. D.; Chou, M. Y.; Cohen, M. L. *Solid State Phys.* **1987**, *40*, 94.
(7) Borg, X. *Magic Numbers Derived from Variable Phase Nuclear Model*; Blaze Labs Research: 2006.
(8) Pradhan, P.; Ray, A. K. *J. Mol. Struct.* **2004**, *716*, 109.
(9) Mainardi, D. S.; Balbuena, P. B. *Langmuir* **2001**, *17*, 2047.
(10) Mainardi, D. S.; Balbuena, P. B. *Int. J. Quantum Chem.* **2001**, *85*, 580.
(11) Mainardi, D. S.; Balbuena, P. B. *J. Phys. Chem. A* **2003**, *107*, 10370.
(12) Derosa, P. A.; Seminario, J. M.; Balbuena, P. B. *J. Phys. Chem. A* **2001**, *105*, 7917.
(13) Balbuena, P. B.; Derosa, P. A.; Seminario, J. M. *J. Phys. Chem. B* **1999**, *103*, 2830.
(14) Gong, X. G. *Phys. Rev. B* **1997**, *56*, 1091.
(15) Gong, X. G.; Kumar, V. *Phys. Rev. Lett.* **1993**, *70*, 2078.
(16) Gong, X. G.; Kumar, V. *Phys. Rev. B* **1994**, *50*, 17701.
(17) Khanna, S. N.; Jena, P. *Phys. Rev. Lett.* **1992**, *69*, 1664.
(18) Kumar, V.; Bhattacharjee, S.; Kawazoe, Y. *Phys. Rev. B* **2000**, *61*, 8541.
(19) Kumar, V.; Kawazoe, Y. *Phys. Rev. B* **2001**, *64*, 115405.
(20) Kumar, V.; Sundararajan, V. *Phys. Rev. B* **1998**, *57*, 4939.
(21) Seitsonen, A. P.; Laasonen, K.; Nieminen, R. M.; Klein, M. L. *J. Chem. Phys* .**1995**, *103*, 8075.
(22) Seitsonen, A. P.; Puska, M. J.; Alatalo, M.; Nieminen, R. M.; Milman, V.; Payne, M. C. *Phys. Rev. B* **1993**, *48*, 1981.
(23) Rohmer, M.; Wiemann, C.; Munzinger, M.; Guo, L.; Aeschlimann, M.; Bauer, M. *Appl. Phys. A* **2005**, *82*, 87.
(24) Ebehardt, W.; Fayet, P.; Cox, D.; Fu, Z.; Kaldor, A.; Sondericker, D. *Phys. Scr.* **1990**, *41*.
(25) Wang, L. S.; Niu, B.; Lee, Y. T.; Shirley, D. A. *Phys. Scr.* **1990**, *41*, 867.
(26) Cheshnovsky, O.; Uang, S. H.; Pettiette, C. C.; Craycraft, M. J.; Smalley, R. E. *Rev. Sci. Instrum.* **1987**, *58*, 2131.
(27) Ervin, K. M.; Ho, J.; Lineberger, W. C. *J. Chem. Phys.* **1988**, *89*, 4514.
(28) Massobrio, C.; Pasquarello, A.; Car, R. *Phys. Rev. Lett.* **1995**, *75*, 2104.
(29) Binggeli, N.; Chelikowsky, J. R. *Phys. Rev. Lett.* **1995**, *75*, 493.
(30) Muller, J.; Liu, B.; Shvartsburg, A. A.; Ogut, S.; Chelikowsky, J. R.; Siu, K. W. M.; Ho, K. M.; Gantefor, G. *Phys. Rev. Lett.* **2000**, *85*, 1666.
(31) Kietzmann, H.; Morenzin, J.; Bechthold, P. S.; Ganteför, G.; Eberhardt, W.; Yang, D.-S.; Hackett, P. A.; Fournier, R.; Pang, T.; Chen, C. *Phys. Rev. Lett.* **1996**, *77*, 4528.
(32) Akola, J.; Manninen, M.; Hakkinen, H.; Landman, U.; Li, X.; Wang, L. S. *Phys. Rev. B* **1999**, *60*, R11297.
(33) Akola, J.; Manninen, M.; Hakkinen, H.; Landman, U.; Li, X.; Wang, L. S. *Phys. Rev. B* **2000**, *62*, 13216.
(34) Jensen, F. *Introduction to Computational Chemistry*; Wiley: Chichester, U. K., 1999.
(35) Knickelbein, M. B. *Annu. Rev. Phys. Chem.* **1999**, *115*, 50.
(36) Nakatsuji, N.; Nakai, H.; Hada, M. Catalytic Reactions of Transition Metal Clusters and Surfaces from Ab Initio Theory. In *Metal−Ligand Interactions: From Atoms, to Clusters, to Surfaces*; Salahub, D. R., Russo, N., Eds.; Kluwer Academic: Dordrecht, The Netherlands, 1992; p 251.
(37) Tomanek, D.; Schulter, M. A. *Phys. Rev. Lett.* **1991**, *67*, 2331.
(38) Ray, A. K. *J. Phys. B* **1987**, *20*, 5233.
(39) Martin, J. M. L. *J. Chem. Phys.* **1995**, *102*, 8270.
(40) Raghavachari, K.; Binkley, J. S. *J. Chem. Phys.* **1987**, *87*, 2191.
(41) Martin, J. M. L.; Francois, J. P.; Gijbels, R. *J. Chem. Phys.* **1991**, *95*, 9420.
(42) Jones, R. O.; Seifert, G. *Phys. Rev. Lett.* **1997**, *79*, 443.

(43) Jones, R. O. *J. Chem. Phys.* **1999**, *110*, 5189.
(44) Martin, J. M. L.; Taylor, P. R. *J. Phys. Chem. A* **1996**, *100*, 6047.
(45) Joswig, J. O.; Springborg, M.; Seifert, G. *Phys. Chem. Chem. Phys.* **2001**, *3*, 5130.
(46) Belbruno, J. J.; Tang, Z. C.; Smith, R.; Hobday, S. *Mol. Phys.* **2001**, *99*, 957.
(47) Duncan, M. A. *J. Cluster Sci.* **1997**, *8*, 239.
(48) Sun, S.; Cao, Y.; Sun, Z.; Tang, Z.; Zheng, L. *J. Phys. Chem. A* **2006**, *110*, 8064.
(49) Largo, A.; Redondo, P.; Barrientos, C. *J. Phys. Chem. A* **2002**, *106*, 4217.
(50) Presilla-Márquez, J. D.; Graham, W. R. M. *J. Chem. Phys.* **1994**, *100*, 181.
(51) Chen, M. D.; Li, X. B.; Yang, J.; Zhang, Q. E. *J. Phys. Chem. A* **2006**, *110*, 4502.
(52) Zhang, C. *J. Mol. Struct.* **2006**, *759*, 201.
(53) Chen, M. D.; Li, X. B.; Yang, J.; Zhang, Q. E.; Au, C. T. *Int. J. Mass Spectrom.* **2006**, *253*, 30.
(54) Klein, J.; Middleton, R. *Nucl. Instrum. Methods Phys. Res., Sect. B* **1999**, *1*−*2*, 8.
(55) Guo, B. C.; Kerns, K. P.; Castleman, A. W., Jr. *Science* **1992**, *255*, 1411.
(56) Guo, B. C.; Wei, S.; Purnell, J.; Buzza, S.; Castleman, A. W., Jr. *Science* **1992**, *256*, 515.
(57) Wei, S.; Guo, B. C.; Purnell, J.; Buzza, S.; Castleman, A. W., Jr. *Science* **1992**, *256*, 818.
(58) Gueorguiev, G. K.; Pacheco, J. M. *Phys. Rev. B* **2003**, *68*, 241401.
(59) Dance, I. *J. Chem. Soc., Chem. Commun.* **1992**, 1779.
(60) Grimes, R. W.; Gale, J. D. *J. Chem. Soc., Chem. Commun.* **1992**, 1222.
(61) Pauling, L. *Molecular Structure of Ti_8C_{12} and Related Complexes*; National Academy of Sciences: 1992.
(62) Chu, Q.; Li, B.; Yu, J. *J. Mol. Struct.: THEOCHEM* **2007**, *806*, 67.
(63) Millar, T. J.; Leung, C. M.; Herbst, E. *Astron. Astrophys.* **1987**, *183*, 109.
(64) Iijima, S. *Nature* **1991**, *354*, 56.
(65) Kroto, H. W.; Heath, J. R.; Obrien, S. C.; Curl, R. F.; Smalley, R. E. *Nature* **1985**, *318*.
(66) Schimmel, H. G.; Kearley, G. J.; Nijkamp, M. G.; Visser, C. T.; De Jong, K. P.; Mulder, F. M. *Chem.*−*Eur. J.* **2003**, *9*, 4764.
(67) Türker, L. *Int. J. Hydrogen Energy* **2003**, *28*, 223.
(68) Türker, L. *J. Mol. Struct.* **2005**, *723*, 105.
(69) Zhu, Z. H.; Lu, G. Q.; Smith, S. C. *Carbon* **2004**, *42*, 2509.
(70) Viswanathan, B.; Sankaran, M.; Scibioh, M. A. *Bull. Catal. Soc. India* **2003**, *2*, 12.
(71) Türker, L.; Gümüs, S. *J. Mol. Struct.* **2005**, *719*, 103.
(72) Türker, L.; Eroglu, I.; Yucel, M.; Gunduz, U. *Int. J. Hydrogen Energy* **2004**, *29*, 1643.
(73) Zuttel, A. *Naturwissenschaften* **2004**, *91*, 157.
(74) Zaluska, A.; Zaluski, L.; Ström-Olsen, J. O. *J. Alloys Compd.* **2000**, *307*, 157.
(75) Dal Toè, S.; Lo Russo, S.; Maddalena, A.; Principi, G.; Saber, A.; Sartori, S.; Spataru, T. *Mater. Sci. Eng., B* **2004**, *108*, 24.
(76) Imamura, H.; Tabata, S.; Shigetomi, N.; Takesue, Y.; Sakata, Y. *J. Alloys Compd.* **2002**, *330*−*332*, 579.
(77) Frisch, M. J.; Trucks, G. W.; Schlegel, H. B.; Scuseria, G. E.; Robb, M. A.; Cheeseman, J. R.; Montgomery Jr, J. A.; Vreven, T.; K. N. Kudin; J. C. Burant; J. M. Millam; S. S. Iyengar; J. Tomasi; V. Barone; B. Mennucci; M. Cossi; G. Scalmani; N. Rega; G. A. Petersson; H. Nakatsuji; M. Hada; M. Ehara; K. Toyota; R. Fukuda; J. Hasegawa; M. Ishida; T. Nakajima; Y. Honda; O. Kitao; H. Nakai; M. Klene; X. Li; J. E. Knox; H. P. Hratchian; J. B. Cross; C. Adamo; J. Jaramillo; R. Gomperts; R. E. Stratmann; O. Yazyev; A. J. Austin; R. Cammi; C. Pomelli; J. W. Ochterski; P. Y. Ayala; K. Morokuma; G. A. Voth; P. Salvador; J. J. Dannenberg; V. G. Zakrzewski; S. Dapprich; A. D. Daniels; M. C. Strain; O. Farkas; D. K. Malick; A. D. Rabuck; K. Raghavachari; J. B. Foresman; J. V. Ortiz; Q. Cui; A. G. Baboul; S. Clifford; J. Cioslowski; B. B. Stefanov; G. Liu; A. Liashenko; P. Piskorz; I. Komaromi; R. L. Martin; D. J. Fox; T. Keith; M. A. Al-Laham; C. Y. Peng; A. Nanayakkara; M. Challacombe; P. M. W. Gill; B. Johnson; W. Chen; M. W. Wong; C. Gonzalez; Pople, J. A. *Gaussian 03*, revision C.02; Gaussian, Inc: Wallingford, CT, 2004.
(78) *Recent Developments and Applications of Modern Density Functional Theory*; Seminario, J. M., Ed.; Elsevier Science Publishers: Amsterdam, 1996; Vol. 4.
(79) Zhao, Y.; Li, N.; Xu, W. G.; Li, Q. S. *J. Phys. Chem. A* **2004**, *108*, 4887.
(80) Zhao, Y.; Li, N.; Xu, W. G.; Li, Q. S. *Int. J. Quantum Chem.* **2007**, *107*, 81.
(81) Martin, J. M. L.; El-Yazal, J.; Francois, J. P. *Chem. Phys. Lett.* **1996**, *252*, 9.
(82) Pacchioni, G.; Koutecký, J. *Chem. Phys.* **1982**, *71*, 181.
(83) Beyer, M. K.; Kaledin, L. A.; Kaledin, A. L.; Heaven, M. C.; Bondybey, V. E. *Chem. Phys. Lett.* **2000**, *262*, 15.
(84) Koch, W.; Holthausen, M. C. *A Chemist's Guide to Density Functional Theory*, 2nd ed.; Wiley-VCH: 2001.
(85) *Handbook of Chemistry and Physics*, 71st ed.; Lide, D. R., Ed.; CRC Press: Boca Raton, FL, 1991; p 9.
(86) Taylor, J. R. *An Introduction to Error Analysis: The Study of Uncertainties in Physical Measurements*, 2nd ed.; University Science Books: 1996.
(87) Song, B.; Yao, C. H.; Cao, P. L. *Phys. Rev. B* **2006**, *74*, 035306.